New Hyperbranched Polymers for Membranes of High-Temperature Polymer Electrolyte Membrane Fuel Cells: Determination of the Crystal Structure and Free-Volume Size

Sambhu Bhadra,[1] C. Ranganathaiah,[2] Nam Hoon Kim,[3] Seong-Il Kim,[4] Joong Hee Lee[1,3,5]

[1]*BIN Fusion Research Team, Department of Polymer and Nano Engineering, Chonbuk National University, Duckjin-Dong 1Ga 664-14, Jeonju, Jeonbuk 561-756, Republic of Korea*
[2]*Department of Studies in Physics, University of Mysore, Manasagangotri, Mysore 570 006, India*
[3]*Department of Hydrogen and Fuel Cell Engineering, Chonbuk National University, Duckjin-Dong 1Ga 664-14, Jeonju, Jeonbuk 561-756, Republic of Korea*
[4]*Department of Technology Education, Daebul University, Jeonnam 525-702, Republic of Korea*
[5]*World Class University Program, Department of BIN Fusion Technology, Chonbuk National University, Jeonju, Jeonbuk 561-756, Republic of Korea*

Received 25 June 2010; accepted 17 October 2010
DOI 10.1002/app.33637
Published online 25 February 2011 in Wiley Online Library (wileyonlinelibrary.com).

ABSTRACT: The key requirements for a membrane in polymer electrolyte membrane fuel cells are a high ion conductivity, mechanical strength, and barrier properties. We reported earlier on two new promising hyperbranched polymers: poly(benzimidazole-*co*-aniline) (PBIANI), with a uniform rectangular net structure, and poly(benzimidazole-*co*-benzene) (PBIB), with a honeycomb structure. Both polymers exhibit a high ion conductivity and mechanical strength and have proven themselves suitable for the membranes of high-temperature polymer electrolyte membrane fuel cells. In this article, we deal with the determination of crystal structure and free-volume cell/microvoid size of these two polymers. Both PBIANI and PBIB had the same *d*-spacing (3.5 Å). However, the percentage of crystallinity was higher and the crystallite size was larger for PBIB. The kinetic diameters of hydrogen (2.89 Å), oxygen (3.46 Å), water (2.60 Å), and methanol (~ 4.00 Å) were much larger than the free-volume cell/microvoid diameters of PBIANI (1.81 Å) and PBIB (1.96 Å) but much smaller than those of Nafion 115 (6.54 Å) and polybenzimidazole (PBI) (~ 6.00 Å). The very small free-volume sizes of PBIANI and PBIB ensured good barrier properties against hydrogen, oxygen, water, and methanol, unlike those of Nafion- and PBI-type membranes. J Appl Polym Sci 121: 923–929, 2011

Key words: charge transfer; conducting polymers; hyperbranched; membranes; X-ray

INTRODUCTION

The key requirements for a membrane in polymer electrolyte membrane fuel cells (PEMFCs) are a high ion conductivity, good mechanical strength, and low permeability of fuel (hydrogen/methanol), gas (oxygen/air), and water.[1–3] Nafion is the most common material for PEMFC membranes, but it has several disadvantages. For example, it cannot be operated under dry conditions, and at high temperatures (>100°C), there is an issue of water management under humid conditions; it also has inadequate barrier properties. The other challenges with Nafion membranes are its critical system design and operation with respect to water management, a low tolerance for fuel impurities, and the poisoning of the electrode by carbon monoxide.[1–5]

To resolve the aforementioned problems, recent research in PEMFCs has focused mainly on the development of high-temperature polymer electrolyte membrane fuel cell (HT-PEMFC) membranes that operate well above 100°C.[6–8] As reported previously, the phosphoric acid doped polybenzimidazole (PBI) membrane is the most preferred basic polymer membrane for HT-PEMFCs and can be operated at 100–220°C without humidity.[7,8] The operation of a fuel cell at higher temperatures ensures a higher efficiency, high power density, reduced sensitivity to carbon monoxide poisoning of the electrode, and

Correspondence to: J. H. Lee (jhl@chonbuk.ac.kr).
Contract grant sponsor: National Space Lab; contract grant number: S108A01003210.
Contract grant sponsor: World Class University; contract grant number: R31-2008-20029.
Contract grant sponsor: Human Resource Training Project for Regional Innovation through the National Research Foundation of Korea funded by the Ministry of Education, Science and Technology.

TABLE I
Uptake of Phosphoric Acid, Mechanical Strength, and Ion Conductivity of Different Membranes

Sample	Uptake of phosphoric acid (wt %)	Stress at break (MPa)	Ion conductivity (S/cm)	Reference
Nafion 115	Not applicable	28 ± 2	145 ± 2[a]	26
PBIANI	45	26 ± 3	167 ± 2[a]	25
PBIB	14	29 ± 3	92 ± 2[a]	26
PBI	162	3.4	33[b]	12

[a] Ion conductivity was measured at 120°C and at 100% relative humidity.
[b] Conductivity was measured at 150°C by the four-point probe method.

better controllability (because of the absence of water management issues in the membrane).[6,9,10] However, PBI-type membranes cannot comprehensively protect the permeation of fuel.[11] PBI-type membranes are doped with an excess of phosphoric acid to increase their ion conductivity. However, the ion conductivity of PBI-type membranes is still lower than that of a Nafion membrane. Moreover, with increasing degree of doping, the mechanical strength of PBI-type membranes deteriorates abruptly.[12,13] Apart from doping, the ion conductivity of PBI-type membranes has been improved by the addition of inorganic fillers, such as imidazole-containing silica[14] and phosphomolybdic acid,[15] or by sulfonation with sulfuric acid, chlorosulfonic acid, sulfur trioxide, acetylsulfate, and alkylsulfonic acid.[16] However, the addition of inorganic fillers increases the free-volume size of the polymers and enhances the gas permeability of the membrane; this has a deleterious effect on the fuel cell operation.[17] The thermal stability of PBI deteriorates with increasing degree of sulfonation.[16] The barrier properties of PBI-type membranes against fuel also decrease after sulfonation.[18]

The mechanical strength of PBI-type membranes has been improved by the addition of inorganic fillers,[10] preparation of polymeric acid–base blend membranes (referred to as *ionic crosslinking*),[19] covalent crosslinking by thermal treatment,[20] and chemical crosslinking with different crosslinkers (e.g., 3,4-dichlorotetrahydrothiophene-1,1-dioxide,[21] *p*-xylene dichloride,[22] *p*-xylene dibromide,[23] dichloromethyl phosphinic acid[24]). There have been no reports on simultaneous improvements in the ion conductivity, mechanical strength, and barrier properties of PBI-type membranes.

Earlier we reported two new promising hyperbranched polymers: poly(benzimidazole-*co*-aniline) (PBIANI), with a uniform rectangular net structure,[25] and poly(benzimidazole-*co*-benzene) (PBIB), with a honeycomb structure.[26] These two polymers exhibited very good ion conductivity and mechanical strength, comparable with Nafion. The deterioration of the mechanical strength after doping was marginal, unlike in PBI-type membranes. Additionally, PBIANI and PBIB membranes were operable without humidity, unlike Nafion membranes. A summary of a few important previously reported results on PBIANI and PBIB and their comparison with normal PBI and Nafion 115 are presented in Table I. However, in our previous article, we did not report on the barrier properties and crystal structures of these two polymers. The structures of PBIANI and PBIB are closely packed and highly ordered because of interlinking; these structures were expected to improve the barrier properties by reducing the free-volume cell/microvoid size in the polymer structure.

In this article, we report the barrier properties from free-volume measurement and the crystal structure from X-ray diffraction (XRD) analysis for PBIANI and PBIB.

EXPERIMENTAL

Synthesis of PBIANI and PBIB

PBIANI was synthesized in two steps, as presented schematically in Figure 1. 5-Aminoisophthalic acid (AIPA) was first polymerized to poly(5-aminoisophthalic acid) (PAIPA) by oxidative polymerization. PBIANI was then synthesized by the condensation polymerization of PAIPA and 3,3′-diaminobenzidine (DAB).

PBIB was synthesized by the condensation polymerization of trimesic acid (TMA) and DAB. Figure 2 shows a schematic diagram for the synthesis of PBIB.

The detailed synthetic procedure for both polymers can be found elsewhere.[25,26]

Characterization

The XRD study (D/MAX 2500V/PC, Rigaku Americas Corp., Tokyo, Japan) was performed with a copper target (Cu Kα) with a wavelength of 1.5418 Å.

Positron lifetime spectroscopy (PLS) was used to determine the free-volume cell/microvoid size of these polymers. PLS measurements were carried out with a fast–fast coincidence positron annihilation lifetime (PAL) spectrometer consisting of KL-236

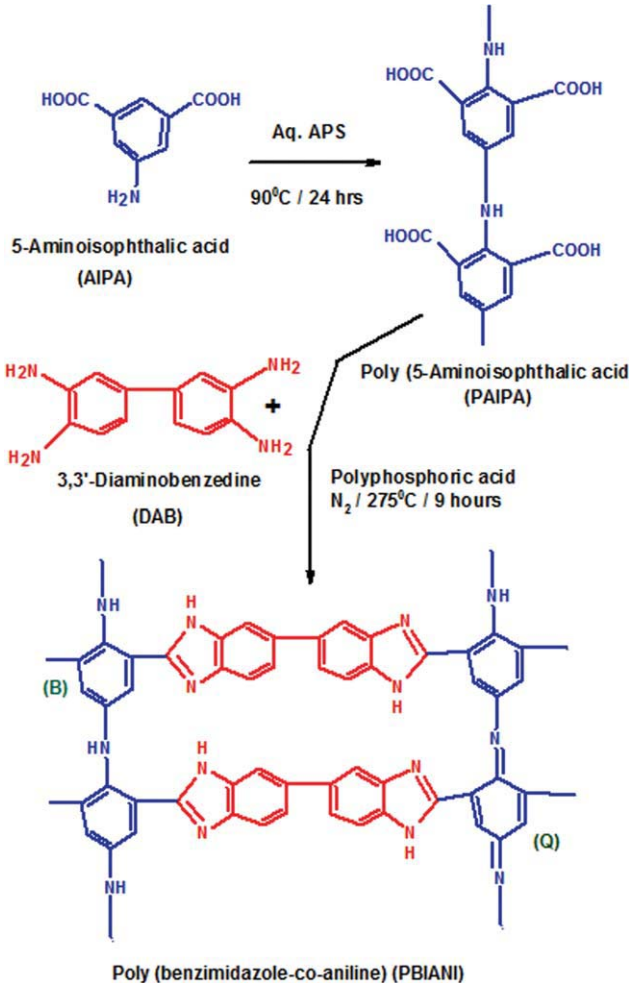

Figure 1 Schematic diagram of the synthesis of PBIANI. In the first step, PAIPA was synthesized by the oxidative polymerization of AIPA with ammonium persulfate (APS) as an oxidizing agent. In the second step, PBIANI was synthesized by the condensation polymerization of PAIPA and DAB. Q represents the quinoid ring, and B represents the benzenoid ring. [Color figure can be viewed in the online issue, which is available at wileyonlinelibrary.com.]

plastic scintillators coupled to RCA-8575 photomultiplier tubes (type XP2020/Q) as detectors. A 17-μCi ^{22}Na positron source, which was deposited onto 0.127 mm thick Kapton foil and sandwiched between two discs of the sample, was placed between two scintillators. The samples used in the PLS measurements were about 1 mm thick discs prepared by solution casting. The positron lifetimes were measured at room temperature and ambient pressure. Several measurements were made for each sample to confirm the reproducibility of the spectrometer. Normally, each spectrum contained more than 10^6 counts, which accumulated in approximately 1.5 to 2 h.[27] The measured lifetime spectra were analyzed by the computer program PATFIT88, and the free-volume cell sizes were calculated with the conventional method.[28,29]

RESULTS AND DISCUSSION

XRD analysis

The degree of crystallinity (a percentage) was calculated from the ratio of the crystalline peak area to the total peak area in the XRD pattern.[30]

The *d*-spacing (Å) corresponding to the crystalline peak was determined by the Debye–Scherrer (powder) method with Bragg's relation:[31]

$$n\lambda = 2d \sin\theta \quad (1)$$

where n is an integer; λ is the wavelength of the X-rays, which is 1.5418 Å for a Cu target; and θ is the angle between the incident and reflected rays.

The crystallite size (t; Å) was determined from the Scherrer relation:[32]

$$t = \frac{K\lambda}{B\cos\theta} \quad (2)$$

where K is the shape factor for the average crystallite (~ 0.9) and B is the full width at half-maximum of the crystalline peak (rad).

Figure 3 presents the XRD patterns of PBIANI and PBIB. The phase in which the polymer chains are parallel and arranged in an orderly manner is known as the *crystalline phase,* which exhibits strong and sharp crystalline peaks in the XRD pattern. On the other hand, the phase where the chains are not arranged in an orderly manner and do not have parallel alignment is known as the *amorphous phase.* The amorphous phase exhibits a shallow and broad peak in the XRD pattern.[33] From the XRD patterns of PBIANI and PBIB, we concluded that the polymers were semicrystalline in nature with a crystalline peak located at $2\theta = 25.2^\circ$ for both of the polymers. The crystalline peak of PBIB [Fig. 3(b)] was stronger and sharper than that of PBIANI [Fig. 3(a)]. Table II lists the percentage of crystallinity, *d*-spacing, and crystallite size of both polymers. Both PBIANI and PBIB had the same *d*-spacing (3.5 Å). However, the percentage crystallinity of PBIB was much higher and the crystallite size of PBIB was much larger compared to those of PBIANI. The crystallinity and crystallite size concurrently increased with increasing degree of regularity in the polymer chains.[30] The higher crystallinity and crystallite size in PBIB indicated that the polymer chains in this polymer were more orderly than those of PBIANI.

Free-volume analysis

The barrier properties of polymeric materials is strongly dependent on their molecular architecture and the presence of free volume or microvoids. If the free-volume cell/microvoid size in a polymer is

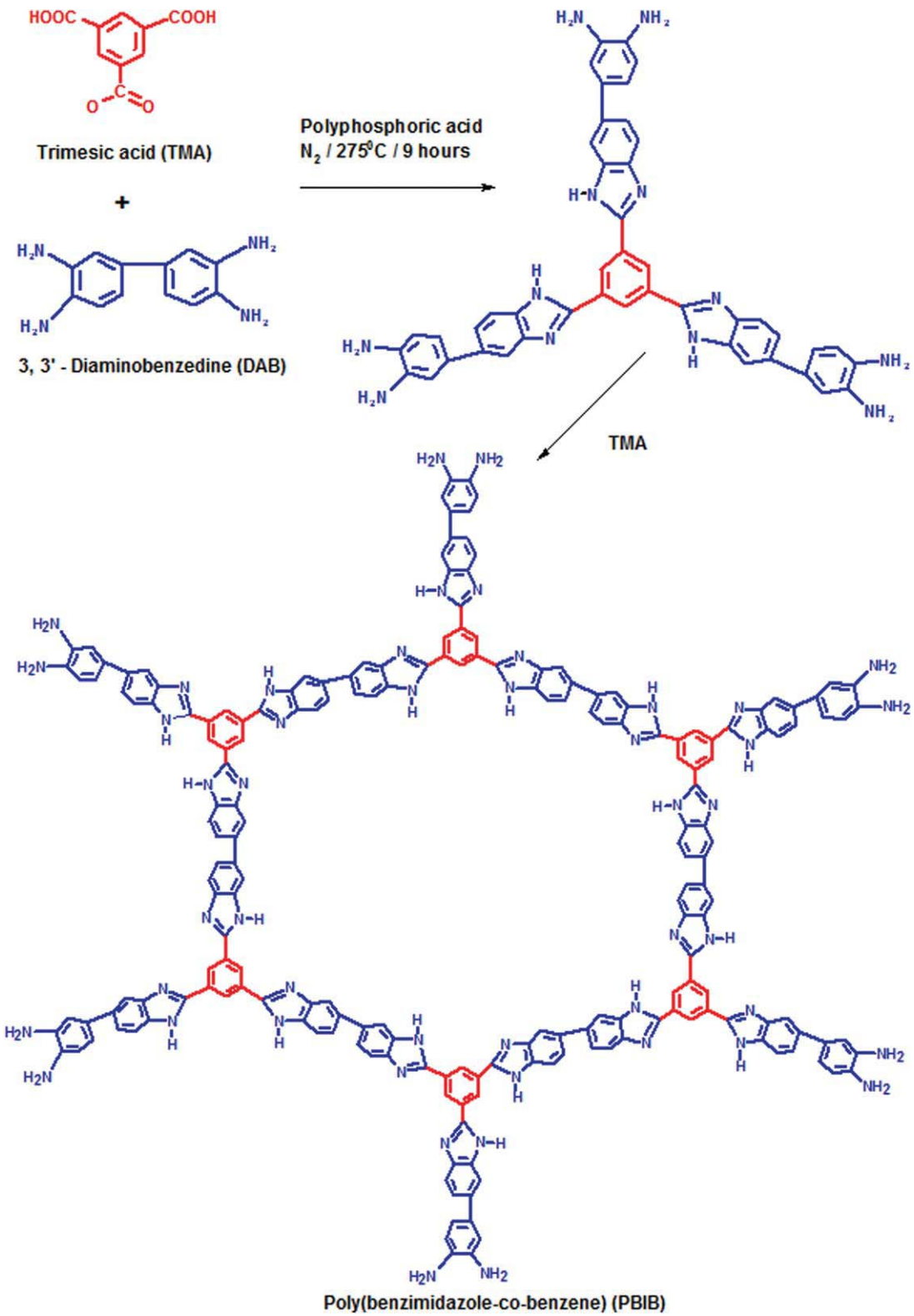

Figure 2 Schematic diagram of the synthesis of PBIB by the condensation polymerization of DAB and TMA. [Color figure can be viewed in the online issue, which is available at wileyonlinelibrary.com.]

larger, the barrier efficiency of the membrane against different molecules will be inferior.[34] The free-volume cell/microvoid size of these polymers was determined by PLS. In PLS, a positron from a radio-active source (Na-22), when injected into a molecular medium, such as a polymer, interacts with the medium and loses its kinetic energy in a very short time and is converted to thermal energy. The

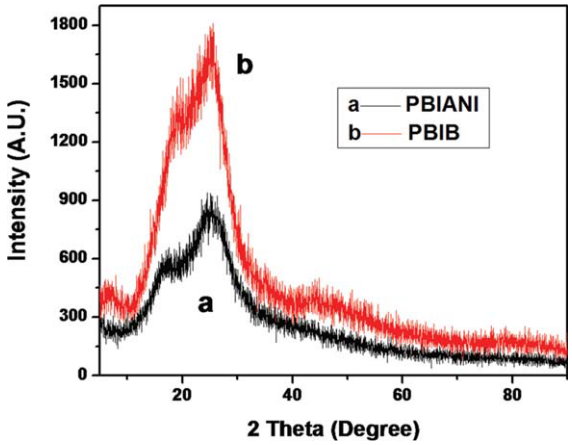

Figure 3 XRD patterns of (a) PBIANI and (b) PBIB. [Color figure can be viewed in the online issue, which is available at wileyonlinelibrary.com.]

thermalized positron may pick up an electron from the medium and be annihilated as a free positron or get trapped in defects present in the crystalline and crystalline–amorphous interface regions of the system and then be annihilated or form a bound state with an electron of the medium (e^+e^-), called the *positronium* (Ps). Ps exists in two allowed spin states: *para*-Ps, in which the spins of e^+ and e^- are aligned antiparallel and which is annihilated into two γ photons with a lifetime of 0.125 ns, and *ortho*-positronium (*o*-Ps), in which the spins are parallel and which is annihilated with a lifetime of 140 ns in free space. However, in molecular media such as polymers, the positron of *o*-Ps picks up an electron from the surrounding medium and is annihilated through a fast channel (this is called *pickoff annihilation*), and its lifetime gets shortened to few nanoseconds. The fact that *o*-Ps preferentially localizes in the free-volume holes of polymers from which it is annihilated makes it the microprobe of free-volume holes because its lifetime and intensity are related to the free-volume size and its content.[28] As such, these measurements have been widely used over the last few decades in the study of the microstructural behavior of polymers and polymer-based systems.

The longest lived component (τ_3) with intensity I_3 is due to the pickoff annihilation of *o*-Ps from the free-volume sites present mainly in the amorphous regions of the polymer matrix.[28] The following relation was used to calculate the free-volume cell radius:[27]

$$(\tau_3)^{-1} = 2\left[1 - \frac{R}{R_o} + \frac{1}{2\pi}\sin\left(\frac{2\pi R}{R_o}\right)\right] ns^{-1} \qquad (3)$$

where $R_o = R + \delta R$ and δR is a fitting parameter. To obtain this fitting parameter, τ_3 values for known hole sizes in porous materials such as zeolite were fitted to eq. (3), and a value of $\delta R = 0.166$ nm was obtained.

It is assumed that *o*-Ps resides in a simple potential well, such as a spherical well of radius R having an infinite potential barrier, δR is the thickness ~0.166 nm of the electron layer that constitutes the wall of the hole and can overlap with the *o*-Ps wave function and ns is nano-second.

The analyzed results for PBIANI and PBIB indicated that the microvoids or free-volume cells were too small for the formation and localization of Ps atoms. Therefore, the second lifetime component (τ_2) from the two-lifetime component analysis, which was caused by the positron annihilation at the defect sites (microvoids) in the polymer matrix, was used to calculate the microvoid size in the PBIANI and PBIB. It is important to note that, experimentally, the standard deviation of τ_2 was very small; this was the result of the exceptionally high intensity of τ_2.

τ_2 in each sample corresponds to the positrons that are trapped at the potential defects (free-volume cells) in the polymer matrix. These free-volume cells result from fluctuations in the packing density and morphology of the polymer chains. As discussed earlier, these free-volume cells are too small for the formation of Ps, the bound state of a positron–electron pair. The positrons were potentially trapped at these smaller free-volume cells, and they subsequently were annihilated there. The radius (R; nm) of the microvoids/free-volume cells corresponding to the trapped positron lifetime (τ_2; ns) are related as follows:[29]

$$(\tau_2)^{-1} = 4\left[1 - \frac{R}{R_o} + \frac{1}{2\pi}\sin\left(\frac{2\pi R}{R_o}\right)\right] ns^{-1} \qquad (4)$$

A detailed discussion of this modification of the conventional relation can be found elsewhere.[29]

Figure 4 shows the kinetic diameters of hydrogen (2.89 Å), oxygen (3.46 Å), water (2.60 Å), and methanol (~ 4.00 Å) along with the free-volume cell/microvoid sizes of the Nafion 115 (6.54 Å), PBIANI (1.81 Å), PBIB (1.96 Å), and PBI (~ 6.00 Å). The kinetic diameters of hydrogen, oxygen, water, and methanol and the free-volume cell size of PBI were reproduced from other reports,[35–37] and the free-volume cell sizes of Nafion 115, PBIANI, and PBIB were determined from the PLS measurements. The microvoid diameters of PBIANI and PBIB were much smaller than those of Nafion 115 and PBI because of the closely packed and highly ordered

TABLE II
Percentage of Crystallinity, *d*-Spacing, and Crystallite Size of the PBIANI and PBIB

Sample	Crystallinity (%)	*d*-spacing (Å)	Crystallite size (Å)
PBIANI	33	3.5	12.3
PBIB	47	3.5	24.1

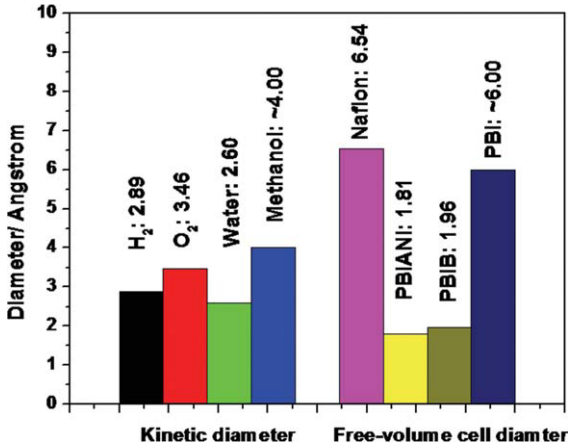

Figure 4 Kinetic diameters of hydrogen, oxygen, water, and methanol along with the free-volume cell/microvoid diameters of Nafion 115, PBIANI, and PBIB. [Color figure can be viewed in the online issue, which is available at wileyonlinelibrary.com.]

structures of PBIANI and PBIB. The kinetic diameters of hydrogen, oxygen, water, and methanol were much larger than the microvoid diameters of PBIANI and PBIB. As a result, we expected that the PBIANI and PBIB membranes would prevent the permeation of these molecules. On the other hand, the kinetic diameters of hydrogen, oxygen, water, and methanol were much smaller than the free-volume cell diameters of Nafion 115 and PBI. This suggested that these molecules would permeate easily through the Nafion 115 and PBI membranes. Therefore, fuel (hydrogen/methanol) crossover, the issue of water management, and the formation of hydrogen peroxide due to the diffusion of oxygen could be stopped or diminished greatly with PBIANI and PBIB membranes.

CONCLUSIONS

PBIANI, with an uniform rectangular net structure, and PBIB, with a honeycomb structure, were found to be promising for the membranes of HT-PEMFCs.

Both PBIANI and PBIB had the same *d*-spacing (3.5 Å). However, the percentage of crystallinity was much higher and the crystallite size was much larger for PBIB compared to PBIANI; this indicated that the polymer chains in PBIB were more ordered than those of PBIANI.

The kinetic diameters of hydrogen (2.89 Å), oxygen (3.46 Å), water (2.60 Å), and methanol ($\sim$ 4.00 Å) were much larger than the free-volume cell/microvoid diameters of PBIANI (1.81 Å) and PBIB (1.96 Å) but were much smaller than those of Nafion 115 (6.54 Å) and PBI ($\sim$ 6.00 Å). As a result, the PBIANI and PBIB membranes prevented the permeation of these molecules but Nafion 115 and PBI membranes did not. Therefore, the PBIANI and PBIB membranes could stop or greatly diminish fuel (hydrogen/methanol) crossover, issues of water management, and the formation of hydrogen peroxide due to oxygen diffusion.

In our earlier study, we found that these two polymers exhibited very good ion conductivity and mechanical strength. In this study, we found that these polymers should have very good barrier properties. Therefore, these polymers exhibited simultaneous improvements in the mechanical properties, ion conductivity, and barrier properties compared to those of PBI-type membranes. Hyperbanching with specific architectures in the PBI-type membranes resulted in simultaneous improvements in the ion conductivity, mechanical strength, and barrier properties, which are the most important requirements for HT-PEMFCs. The improvement in these properties was attributed to the interlinked, closely packed, and highly ordered structure of PBIANI and PBIB. To the best of our knowledge, such simultaneous improvements in these properties have not been exhibited by any other polymer.

References

1. Steele, B. C. H.; Heinzel, A. Nature 2001, 414, 345.
2. Viswanathan, B.; Scibioh, M. A. Fuel Cell Principles and Application: CRC/Taylor & Francis: New York, 2007; p 272.
3. Sopian, K.; Daud, W. R. W. Renew Energy 2006, 31, 719.
4. Iojoiu, C.; Chabert, F.; Marechal, M.; Kissi, N. E.; Guindet, J.; Sanchez, J. Y. J Power Sources 2006, 153, 198.
5. Jagur-Grodzinski, J. Polym Adv Technol 2007, 18, 785.
6. Li, Q.; He, R.; Jensen, J. O.; Bjerrum, N. J. Chem Mater 2003, 15, 4896.
7. Zhang, J.; Xie, Z.; Zhang, J.; Tang, Y.; Song, C.; Navessin, T.; Shi, Z.; Song, D.; Wang, H.; Wilkinson, D. P.; Liu, Z. S.; Holdcroft, S. J Power Sources 2006, 160, 872.
8. Kreuer, K. D. J Membr Sci 2001, 185, 29.
9. Ma, Y. L.; Wainright, J. S.; Litt, M. H.; Sanivel, R. F. J Electrochem Soc 2004, 151, A8.
10. He, R.; Li, Q.; Xiao, G.; Bjerrum, N. J. J Membr Sci 2003, 226, 169.
11. Pu, H.; Liu, Q.; Liu, G. J Membr Sci 2004, 241, 169.
12. He, R.; Che, Q.; Sun, B. Fibers Polym 2008, 9, 679.
13. Lobato, J.; Canizares, P.; Rodrigo, M. A.; Linares, J. J.; Aguilar, J. A. J Membr Sci 2007, 306, 47.
14. Mustarelli, P.; Quartarone, E.; Grandi, S.; Carollo, A.; Magistris, A. Adv Mater 2008, 20, 1339.
15. Asensio, J. A.; Borros, S.; Gomez-Romero, P. Electrochem Commun 2003, 5, 967.
16. Rikukawa, M.; Sanui, K. Prog Polym Sci 2000, 25, 1463.
17. Sadeghi, M.; Semsarzadeh, M. A.; Moadel, H. J Membr Sci 2009, 331, 21.
18. Pu, H.; Liu, Q. Polym Int 2004, 53, 1512.
19. Kerres, J.; Xing, D.; Schonberger, F. JPolym Sci Part B: Polym Phys 2006, 44, 2311.
20. Gillham, J. K. Science 1963, 139, 494.
21. Young, J. S.; Long, G. S.; Gregory, S.; Espinoza, B. F. U.S. Pat. 2006, 6,997,971.
22. Wang, K. Y.; Xiao, Y. C.; Chung, T. S. Chem Eng Sci 2006, 61, 5807.
23. Li, Q.; Pan, C.; Jensen, J. O.; Noye, P.; Bjerrum, N. J. Chem Mater 2007, 19, 350.

24. Noye, P.; Li, Q.; Pan, C.; Bjerrum, N. J. Polym Adv Technol 2008, 19, 1270.
25. Bhadra, S.; Kim, N. H.; Lee, J. H. J Membr Sci 2010, 349, 304.
26. Bhadra, S.; Kim, N. H.; Choi, J. S.; Rhee, K. Y.; Lee, J. H. J Power Sources 2011, 195, 2470.
27. Raj, J. M.; Ranganathaiah, C. Polym Degrad Stab 2009, 94, 397.
28. Jean, Y. C. Microchem J 1990, 42, 72.
29. Singh, J. J. Nucl Instrum Methods Phys Res Sect B 1992, 63, 477.
30. Bhadra, S.; Kim, N. H.; Rhee, K. Y.; Lee, J. H. Polym Int 2009, 58, 1173.
31. Castellan, G. W. Physical Chemistry; Narosa: New Delhi, 1996; p 701.
32. Kennedy, C. J.; Lerber, K. V.; Wess, T. J e-Preserv Sci 2005, 2, 31.
33. Li, C. J.; Ohmori, A.; Harada, Y. J Therm Spray Technol 1996, 5, 69.
34. Wang, J.; Zhang, H.; Jiang, Z.; Yang, X.; Xiao, L. J Power Sources 2009, 188, 64.
35. Shieh, J. H.; Chung, T. S. J Polym Sci Part B: Polym Phys 1999, 37, 2851.
36. Elshof, J. E.; Abadal, C. R.; Sekulic, J.; Roy Chowdhury, S.; Blank, D. H. A. Microporous Mesoporous Mater 2003, 65, 197.
37. Park, H. B.; Jung, C. H.; Lee, Y. M.; Hill, A. J.; Pas, S. J.; Mudie, S. T.; Wagner, E. V.; Freeman, B. D.; Cookson, D. J. Science 2007, 318, 254.